

Original Article

Alpinumisoflavone suppresses tumour growth and metastasis of clear-cell renal cell carcinoma

Tingting Wang¹, Yuhua Jiang², Lei Chu², Tianhui Wu³, Jie You¹

¹Shanghai Ninth People's Hospital, Shanghai JiaoTong University School of Medicine, Shanghai 200011, China;

²Tumor Hospital of Qingdao, Shandong 266042, China; ³Qingdao 5th People's Hospital, Qingdao 266002, Shandong, China

Received January 11, 2017; Accepted January 15, 2017; Epub April 1, 2017; Published April 15, 2017

Abstract: Clear cell renal cell carcinoma (ccRCC) is the most common type of kidney cancer. The present study is aimed to investigate the role of alpinumisoflavone (AIF), a naturally occurring flavonoid compound, in ccRCC and the underlying mechanism. In this study, miR-101 has been identified as a novel therapeutic target, which exerts anti-tumor effect on ccRCC by directly targeting RLIP76. Moreover, our results showed that AIF was able to increase the expression of miR-101 by suppressing Akt signalling. Our findings in this study provided experimental evidence that AIF has the potential to be used as an agent in the treatment of ccRCC.

Keywords: Alpinumisoflavone, clear cell renal cell carcinoma, miR-101, RLIP76

Introduction

Renal cell carcinoma (RCC) is the 7th most common cancer in the developed world and by far the most lethal urologic cancer, representing 80% to 85% cancer of the kidney [1, 2]. Statistics shows that RCC accounts for about 209,000 new cancer cases and 102,000 deaths per year worldwide [3]. The most common histological subtype of RCC is clear-cell renal cell carcinoma (ccRCC), which can be cured with partial or radical nephrectomy at early stage. However, approximately 20-30% of patients have metastatic ccRCC at diagnosis. Moreover, up to 30% of newly diagnosed patients with localized disease develop metastases and among 20-30% post-surgery treatment cases recurrence is eventually noted [4]. During the last decade, a better understanding of ccRCC carcinogenesis has led to the development of novel targeted therapies targeting two interacting pathways: the VHL/HIF/VEGF and the PI3K/AKT/mTOR pathways, improving the prognosis of patients with ccRCC [5-8]. Unfortunately, because of tumor recurrence and metastasis, the clinical outcome has not shown a satisfactory improvement in the last decade despite advances in diagnostic and

therapeutic strategies including introduction of target therapy in clinical practice. Therefore, more understanding in the factors involved in the tumorigenesis process of ccRCC is imperative in order to develop more effective therapeutic strategies against ccRCC.

MicroRNAs (miRNAs), a family of small non-coding RNAs, function as either oncogenes or tumor suppressors and regulate a variety of cellular processes, such as cell differentiation, proliferation, apoptosis, migration and invasion through repressing the expression of target genes [9]. As one of these miRNAs, MiR-101 has been found to play anti-tumour role in a variety of human malignancies, including hepatocellular carcinoma, breast cancer, gastric cancer, lung cancer, colorectal cancer, bladder cancer and prostate cancer [10-16]. However, the role of miR-101 in ccRCC and the mechanism by which miR-101 is regulated in ccRCC remains largely unknown.

As a major active ingredient of a traditional Chinese medicine *Derris eriocarpa* in Southwest part of China, alpinumisoflavone (AIF) possesses a variety of pharmacological activities, including atheroprotective [17], estrogenic [18], anti-

bacterial [19]. More interesting, a couple of studies have showed that AIF can exert anti-tumor effect in vitro [20, 21]. However, little is known about the underlying mechanism of the anti-tumor effect of AIF. Therefore, this study was designed to investigate the anti-tumor effect of AIF on ccRCC and elucidate the underlying mechanism of the anti-tumor effect of AIF. Our results showed that AIF exerted anti-tumor effect in ccRCC both in vitro and in vivo, at least partly, through modulating miR-101/RLIP76 signaling.

Materials and methods

Patients' specimen

47 patients diagnosed with ccRCC and received surgery in Tumor Hospital of Qingdao and Qingdao 5th People's Hospital, were included in this study. In addition to primary tumor tissue, samples belonging to corresponding non-malignant kidney cortex were also collected during surgery from the same kidney as corresponding tumor tissue. The collected tissue was snap frozen and kept in liquid (-70°C) until analysis. All samples were blindly examined by two senior pathologists for diagnosis and histological classification according to the 2011 Union for International Cancer Control TNM classification. The clinical study protocol was reviewed and approved by Medical Ethics Committee of Tumor Hospital of Qingdao and Qingdao 5th People's Hospital and consent forms were signed by all patients or guardians.

RNA isolation and quantitative real-time PCR (qRT-PCR)

Total RNA and miRNA were isolated from patient specimen and corresponding non-malignant kidney cortex using TRIzol Reagent (Life Technology, Carlsbad, CA). Reverse transcription was performed following the manufacturer's instructions. Then qPCR was performed using a Stratagene RNeasy mini kit or RNeasy kit (Qiagen, Hilden, Germany), respectively. Complementary DNA (cDNA) was randomly primed from 2 µg of total RNA using High-Capacity cDNA Reverse Transcription Kit (Applied Biosystems, Foster City, CA, USA). Reverse transcription quantitative PCR (RT-PCR) was subsequently performed in triplicate with QuantiTect SYBR Green PCR Kit (Qiagen, Hilden, Germany). All primers were purchased from Qiagen. Data

were collected and analyzed using the $\Delta\Delta Ct$ (U6-miR-101) for the quantification of the relative mRNA expression level.

Cell culture and cell lines

Human ccRCC cell lines 786-O and Caki1 were purchased from ATCC (Shanghai, China). All cells were cultured at 37°C in a humidified atmosphere of 5% CO₂ in RPMI-1640 medium with 10% (v/v) heat-inactivated FBS, 2 mM glutamine, 1% nonessential amino acids and 100 U/ml streptomycin and penicillin.

Construct of miR-101 mimic or anti-miR-101 and cell transfection

The lentiviral constructs of miR-101 mimic (miR-101), miR-101 control (miR-con), anti-miR-101, and anti-miR control (anti-miR-con) were constructed by Genepharma (Shanghai, China). CRC cells were infected with the constructed lentivirus following standard protocol.

Transfection of RLIP76 overexpressing plasmid

RLIP76 overexpressing plasmid was constructed as previously described using a plasmid vector pGCsi-H1 [22]. The transfection was conducted using Lipofectamine 3000 reagent (Invitrogen, Grand Island, NY) according the manufacturer's instructions. Cells transfected with empty vector were used as controls. 48 hours after transfection, the cells were rinsed before resuspended in fresh culture media and the overexpression was verified by western blot analysis.

Luciferase reporter assay

The molecular target of miR-101 was predicted using the computational algorithm softwares, TargetScan [23] and microRNA.org [24]. The 3' untranslated region (UTR) of RLIP76 was identified as a potential target gene. To verify whether RLIP76 is a direct target of miR-101, a luciferase reporter was constructed by amplifying a wild-type 3'UTR segment of RLIP76 that contains putative miR-101 binding sites and inserting downstream of the luciferase reporter gene in pGL3 vector (Promega, Madison, WI, USA). The primers used to amplify the 3'-UTR of RLIP76 was designed and synthesized by Sangong (Shanghai, China). The mutagenesis of the 3'UTR segment of RLIP76 was performed as previously described [22]. Both wild-type

Alpinumisoflavone suppress renal cell carcinoma

and mutant luciferase reporter constructs were confirmed by sequencing. CRC cells were transiently co-transfected with 0.2 µg of pGL3-RLIP76-3'UTR or pGL3-RLIP76-3'UTR Mut, 0.02 µg of pRL-TK-Renilla luciferase reporter plasmids (Promega, Madison, WI) containing the Renilla-luciferase for normalization, and with 5 pmol of miR-101 mimic or negative control. 48 hours after the transfection, the luciferase activity was examined using a Dual-luciferase assay system (Promega, Madison, WI).

Western blot

The cell lysate (30-50 µg) samples were mixed with 6 × sample buffer, boiled for 5 minutes, electrophoresed in 10% sodium dodecyl sulfate polyacrylamide gel and there after transferred to PVDF membranes. The membrane was then blocked in PBS containing 5% bovine serum albumin (BSA) for 1 hour at room temperature. The membranes were incubated with specific primary antibodies in Tris-buffered saline at 4°C overnight. After washing, the membranes were incubated with HRP-conjugated secondary antibodies (Beyotime Institute of Biotechnology, Shanghai, China). ECL detection reagent (7Sea Biotech., Shanghai, China) was used for blot detection according to the manufacturer's instructions.

Cell viability assay

Cell viability were determined with the 3-[4,5-dimethylthiazol-2-yl]-2,5-diphenyltetrazolium-bromide (MTT, Sigma-Aldrich, St. Louis, MO) assay. Cells were seeded into 96-well plates (5 × 10³ cells/well). Following treatments, cells were incubated with MTT (20 µl/well) at 37°C for 4 h, and then 200 µl DMSO was added into each well. The plates were read in a microplate autoreader (BMG LABTECH, offenburg, Germany) at a wavelength of 570 nm. Each experiment was repeated three times.

Cologenicity formation

Cells suspended in DMEM agarose medium were seeded in each well of a 6-well plate over a bottom layer of solidified DMEM agarose medium. Cultures were maintained for 14 days without fresh medium feeding at 37°C in a humidified atmosphere of 95% air and 5.0% CO₂. Then cell colonies with over 50 cells were

enumerated and stained with violet crystal before being photographed using a digital camera (Olympus, Tokyo, Japan).

Flow cytometry

Following treatment, CRC cells were harvested and stained with Annexin V-PE and propidium iodide using an Apoptosis kit (BD Pharmingen, Franklin Lakes, NJ) according to the manufacturer's instructions. Then the apoptotic percentage of treated cells was determined by a flow cytometer (Beckman Coulter Inc., Miami, FL).

Wound scratch assay

Each well of 24-well tissue culture plate was seeded with cells to a final density of 1 × 10⁵ cells per well and these cells were maintained at 37°C and 5% CO₂ for 24 hours to permit cell adhesion and the formation of a confluent monolayer. These confluent monolayers were then scored with sterile pipette tip to leave a scratch of approximately 0.4-0.5 mm in width. Cell surface was then washed with serum-free culture medium for three times to remove dislodged cells. Wound closure was monitored by collecting digitized images at 0 and 24 hours after the scratch was performed. Digitized images were captured with an inverted microscope (MOTIC CHINA GROUP CO., Xiamen, China) and digital camera (Nikon, Tokyo, Japan). The digitized images were then analyzed using Image-J software.

Invasion assay

24-well Transwells coated with Matrigel (8-µm pore size; BD Biosciences, San Jose, California) were used for cell invasion assays [25]. Equal numbers (1 × 10⁵) cells were plated onto separate well. Cells were starved overnight in serum-free medium, trypsinized and washed three times in DMEM containing 1% FBS. A total of 1 × 10⁵ cells were then resuspended in 500 µl DMEM containing 1% FBS and added to the upper chamber, while MEM with 10% FBS was added to the lower chamber as chemoattractant. For the control, medium containing 1% FBS was added to the lower chamber. After 24 hours of incubation, the Matrigel and the cells remaining in the upper chamber were removed by cotton swabs. The cells on the lower surface of the membrane were fixed in formaldehyde and stained with hematoxylin staining solution.

Alpinumisoflavone suppress renal cell carcinoma

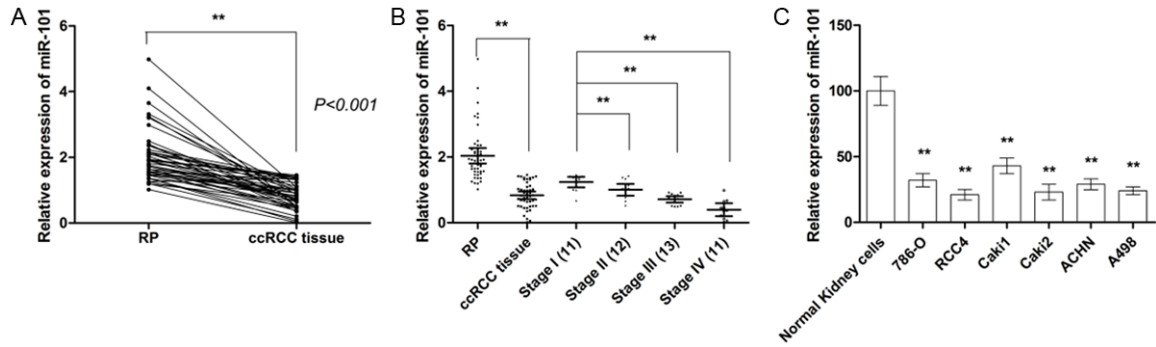


Figure 1. The expression of miR-101 in ccRCC tissues and cell lines. A. The expression of miR-101 in ccRCC tissue is significantly lower compared with RP. B. The expression of miR-101 is associated with TNM stage. C. The expression of miR-101 is significantly lower in ccRCC cell lines compared with normal kidney cells. ** $P < 0.01$.

The cells in at least five random microscopic fields (magnification, $\times 200$) were counted and photographed.

Tumor growth xenograft experiment

The in vivo experiments were performed in accordance with relevant guidelines and regulations for the care and use of laboratory animals, with the approval of the Institutional Animal Care and Use Committee at Tumor Hospital of Qingdao and Qingdao 5th People's Hospital. Male nude mice (BALB/c Nude; 4 weeks old) were obtained from the Shanghai Institute of Material Medical (Chinese Academy of Science). 786-O cells (5×10^6 cells) in 0.1 ml saline were injected subcutaneously into the flanks of nude mice. Tumor size was examined every 3 days and the tumor volumes were calculated according to the following formula: tumor volume = largest diameter \times perpendicular height²/2.

Pulmonary metastasis analysis

To evaluate the effect of AIF on pulmonary metastasis of ccRCC, 786-O cells (1×10^6 cells) in 0.1 ml saline were injected into the tail vein of mice. Mice were sacrificed 12 weeks after inoculation and consecutive sections of the whole lung were subjected to hematoxylin-eosin staining. All of the metastatic lesions in lung were examined and counted to evaluate pulmonary metastasis.

Statistical analysis

Values were presented as the mean \pm SD. The comparison of miR-542-3p levels in tumor and

normal tissue were performed using student's t test. Statistical comparisons between cell lines were performed by one-way ANOVA followed by Dunnett's t-test. GraphPad Prism software (GraphPad Software Inc., La Jolla, CA) was used to analyze experimental data and a P value less than 0.05 was considered to be statistically significant.

Results

The expression of miR-101 is lower in ccRCC tissues compared with renal parenchyma

The level of miR-101 expression was determined by quantitative RT-PCR analysis. as shown in **Figure 1A** and **1B**, the expression of miR-101 was significantly downregulated in tumor tissues relative to corresponding renal parenchyma. Moreover, our results showed that the expression of miR-101 was negatively associated with the tumor stage of ccRCC (**Figure 2B**). To establish the association of miR-101 and clinicopathological features of patients with ccRCC, patients were allocated into two groups with miR-101 at levels less than the median expression level in the low group while and those samples with expression above the median value in the high expression group. Our results showed that miR-101 inversely correlated with TNM stage and distant metastasis ($P < 0.05$, **Table 1**). However, no significant correlation was found between miR-101 levels with other clinicopathological features, such as gender, age and Furman stage. Taken together, our results suggested that miR-101 might play a role in the development and progression of ccRCC.

Table 1. Correlation of miR-101 expression and clinical characteristics in ccRCC patients

Variables	Low miR-101 (n=23)	High miR-101 (n=24)	P-value
Gender			0.6662
Male	11	10	
Female	12	14	
Age			0.6578
≤60	14	12	
>60	9	12	
Tumor size			0.8294
≤4 cm	12	12	
>4 cm	11	12	
Furman grade			0.051
I/II	8	14	
III/IV	15	10	
TNM stage			0.029*
I/II	9	14	
III/VI	14	7	
Distant metastasis			0.030*
No	8	13	
Yes	15	11	

*p<0.05.

MiR-101 is downregulated in ccRCC cell lines and functions as tumor suppressor

The level of miR-101 in ccRCC cell lines was also examined and our results showed that miR-101 was significantly downregulated in ccRCC cell lines compared with normal kidney cells (**Figure 1C**). Next, the effect of miR-101 on cell growth was determined by MTT assay and colony formation. As shown in **Figure 2A** and **2B**, ectopic overexpression by pre-miR-101 was able to significantly inhibit the cell growth of two ccRCC cell lines, RCC4 and 786-O. The flow cytometric analysis also showed that transfection with pre-miR-101 led to significant increase in apoptotic population (**Figure 2C**). To evaluate the role of miR-101 in metastatic behavior of ccRCC cells, migration and invasion assays were also conducted. As shown in **Figure 2D** and **2E**, miR-101 overexpression exhibited marked suppression in both cell migration and invasion. To further demonstrate the role of miR-101 in ccRCC, two mode cell lines were also transfected with anti-miR-101. As shown in **Figure 3A-E**, suppression of endogenous miR-101 resulted in significant enhancement in cell growth, inhibition of apop-

tosis along with increase in cell migration and invasion.

RLIP76 is a direct target of miR-101

To clarify the molecular mechanisms for the effect of miR-101, candidate target genes of miR-101 was searched in bioinformatics database (MicroCosm and Target scan). Give the crucial role of RLIP76 in ccRCC, we postulated that miR-101 might exert anti-tumor effect by regulating the expression of RLIP76. To confirm our postulation, luciferase reporter containing wild type or mutant 3' UTR of RLIP76 was constructed according to the sequence shown in **Figure 4A**. As shown in **Figure 4B**, luciferase activity of the reporter containing wild-type 3'-UTR of RLIP76 was significantly decreased in cells transfected with pre-miR-101 while no significant change in luciferase activity of the reporter containing mutated 3'-UTR was observed, providing direct evidence that RLIP76 was directly targeted by miR-101. To further study the mechanism by which miR-101 regulated the expression of RLIP76, the mRNA and protein expression in ccRCC cells transfected with pre-miR-101 was examined. As shown in **Figure 4C** and **4D**, miR-101 did not significantly change the mRNA expression of RLIP76. In contrast, the protein expression of RLIP76 was significantly repressed by pre-miR-101, suggesting that miR-101 mediated the post-transcriptional regulation of RLIP76 expression. Moreover, the correlation between RLIP76 expression and miR-101 level in patient tissue samples was also examined, which also supported that miR-101 regulated the expression of RLIP76 post-transcriptionally (**Figure 4E** and **4F**).

Ectopic overexpression of RLIP76 compromises the anti-tumor effect of miR-101

To demonstrate the role of RLIP76 in the anti-tumor effect of miR-101, RLIP76 overexpressing vector was constructed (**Figure 5A**). As shown in **Figure 5B-D**, ectopic overexpression significantly attenuated the anti-proliferative and apoptosis-inducing effect of miR-101 on both RCC4 and 786-O cells. In addition, the inhibition on migration and invasion by miR-101 was also reversed by ectopic RLIP76 overexpression (**Figure 5E** and **5F**). Taken together, our results suggested that miR-101 exerted anti-tumour effect, at least in part, by directly repressing RLIP76 expression.

Aluminumisoflavone suppress renal cell carcinoma

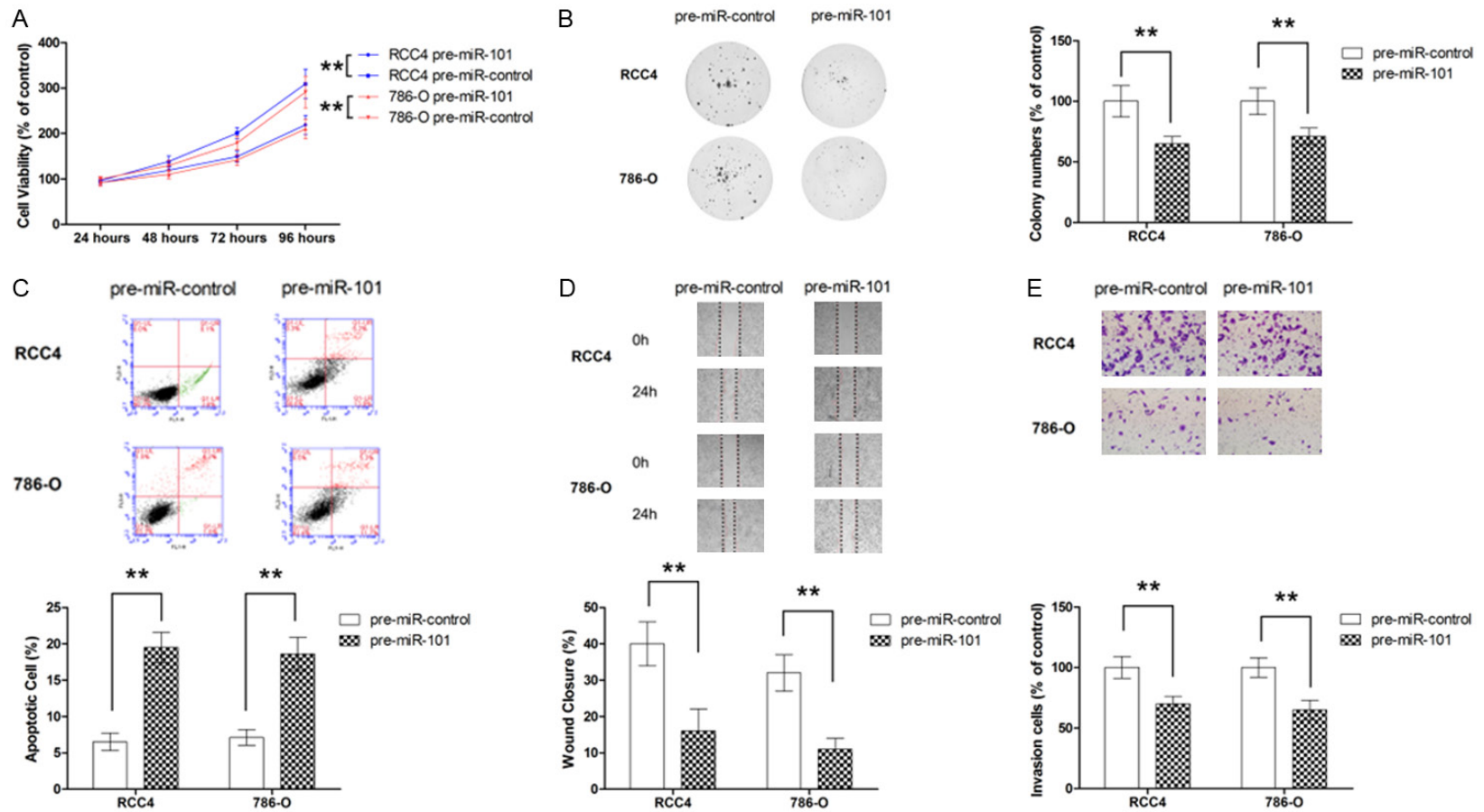


Figure 2. The inhibitory effect of pre-miR-101 on cell growth and invasion. A. Pre-miR-101 inhibits cell growth in vitro. B. Pre-miR-101 suppresses long term cell proliferation. C. Pre-miR-101 induces apoptosis in ccRCC cells. D. Pre-miR-101 inhibits cell migration. E. Pre-miR-101 inhibits cell invasion. **P<0.01.

Aluminumisoflavone suppress renal cell carcinoma

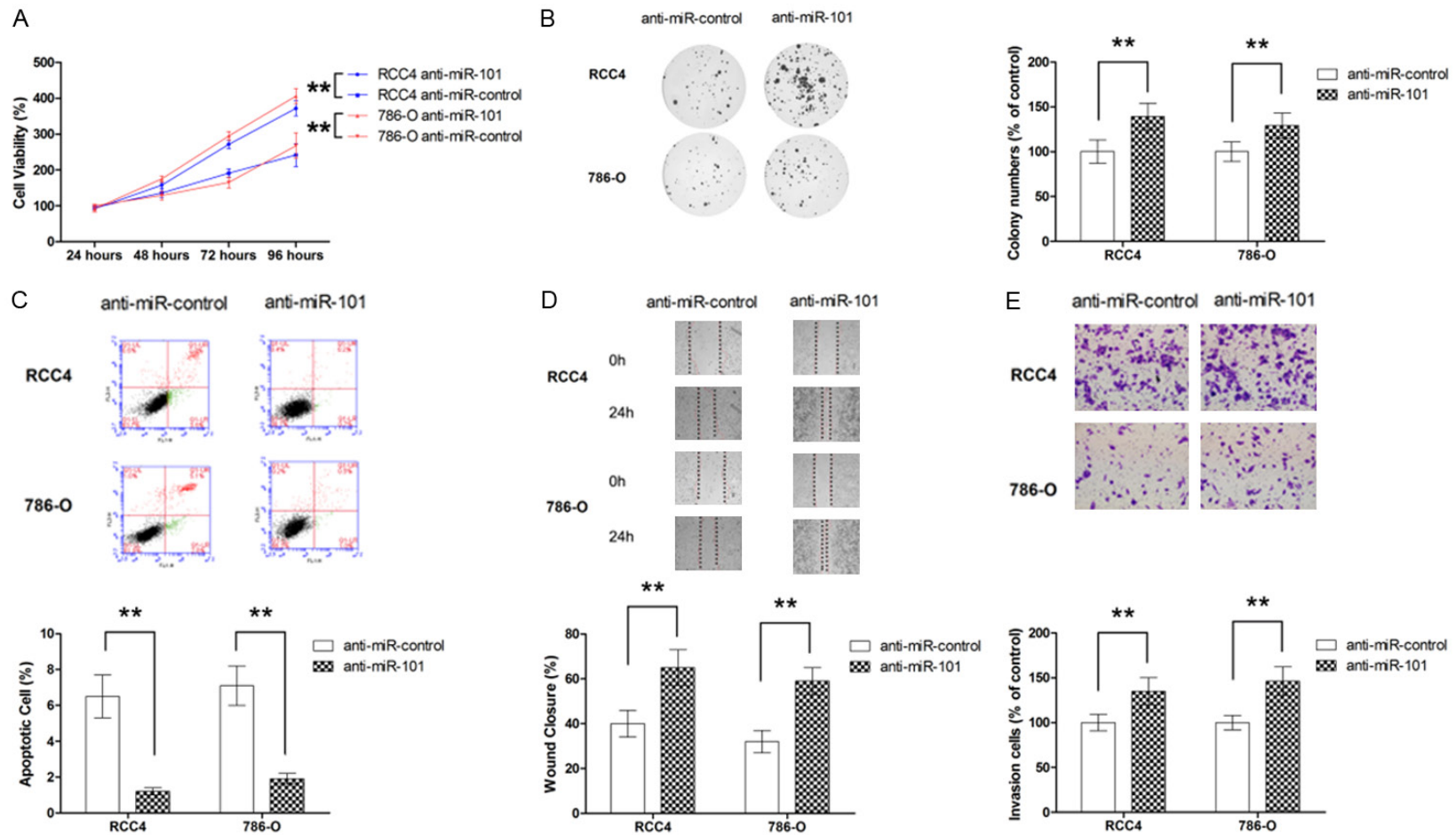


Figure 3. The promoting effect of anti-miR-101 on cell growth and invasion. A. Anti-miR-101 promotes cell growth in vitro. B. Anti-miR-101 enhances long term cell proliferation. C. Anti-miR-101 inhibits apoptosis in ccRCC cells. D. Anti-miR-101 increases cell migration. E. Anti-miR-101 promotes cell invasion. **P<0.01.

Alpinumisoflavone suppress renal cell carcinoma

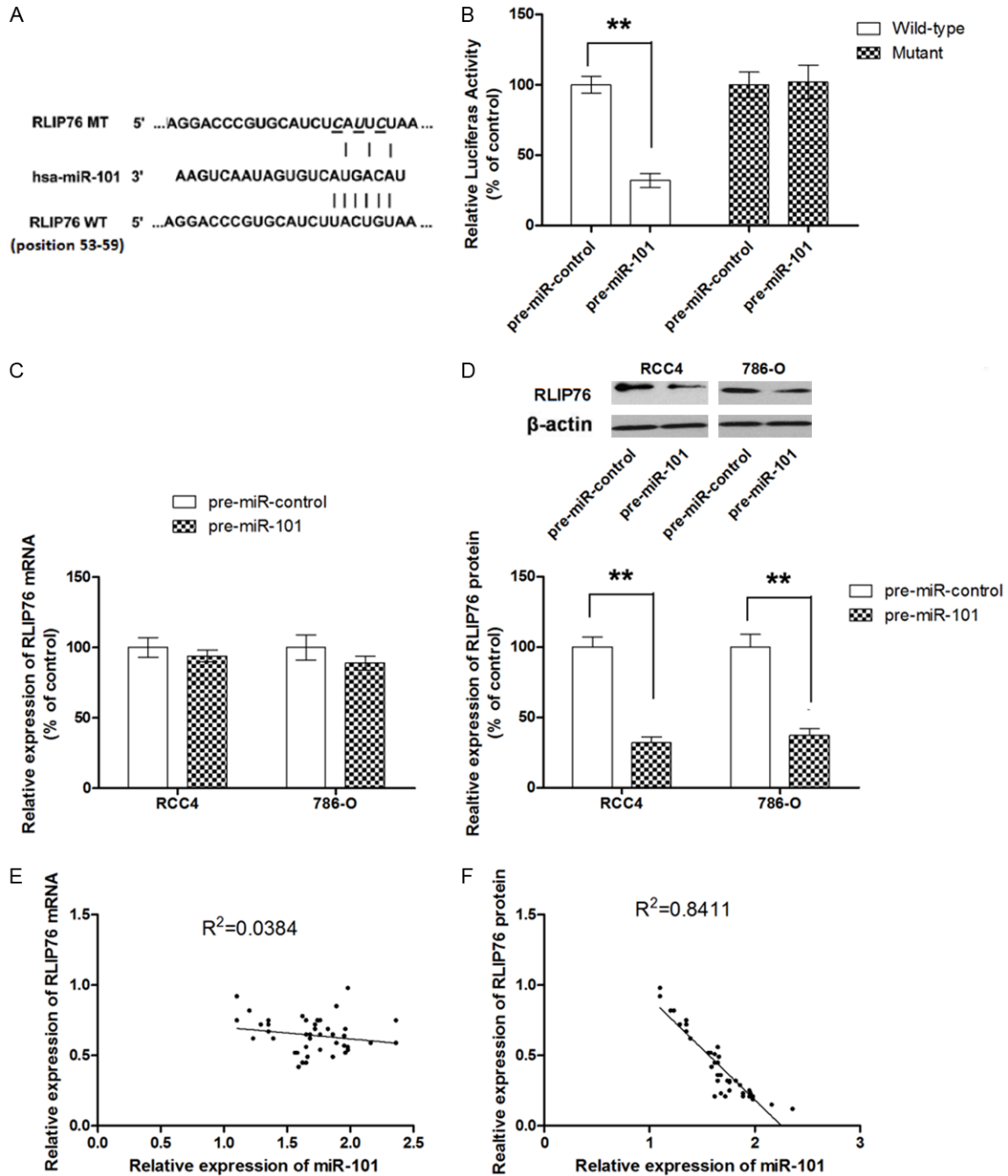


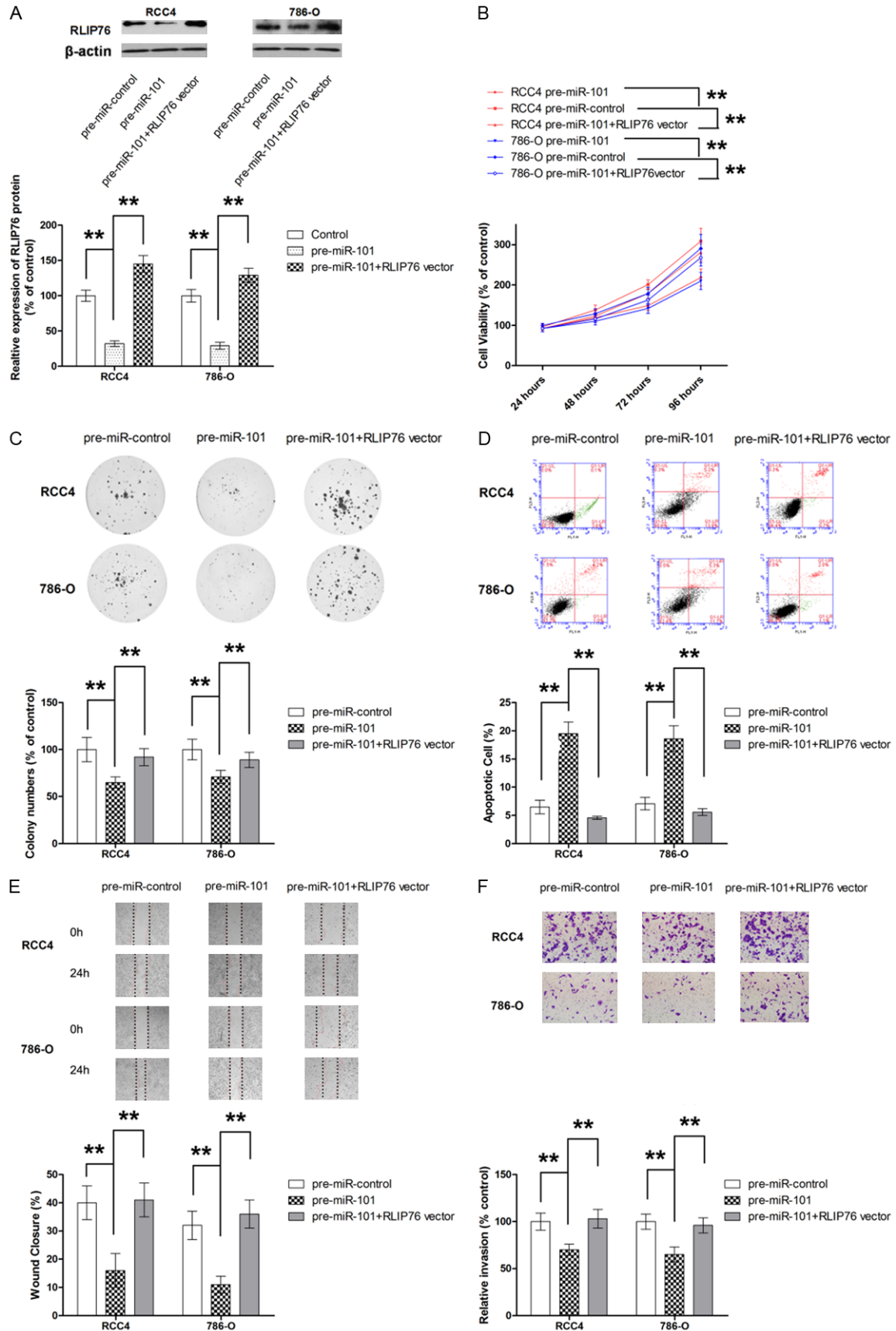
Figure 4. RLIP76 is a direct target of miR-101 in ccRCC cells. A. Schematic illustration of the putative binding sites between wild-type or mutant 3'-UTR of RLIP76 and miR-101. B. Luciferase activity of construct of wild-type RLIP76 is decreased by miR-101 mimic. C. Pre-miR-101 transfection is not associated with changes in RLIP76 mRNA expression in RCC4 and 786-O cells. D. Pre-miR-101 transfection significantly repressed the protein expression of RLIP76. E. The expression level of miR-101 in ccRCC tissue is not associated with RLIP76 mRNA expression. F. The expression level of miR-101 in ccRCC tissue is negatively associated with mRNA expression of RLIP76 in CRC specimen. ** $P < 0.01$.

AIF suppresses cell growth, induces apoptosis and inhibits cell invasion in ccRCC

To appreciate the anti-tumour effect of AIF in RCC, the effects of AIF on various biological

activities of ccRCC cells were examined. As shown in **Figure 6A**, AIF suppressed the cell growth in both tested cell lines in a dose-dependent manner. Our results also showed that AIF treatment was effective in inducing

Aluminumisoflavone suppress renal cell carcinoma



Alpinumisoflavone suppress renal cell carcinoma

Figure 5. RLIP76 mediates the anti-tumor effect of miR-101 in ccRCC cells. A. RLIP76 vector successfully increases the expression of RLIP76 in RCC4 and 786-O cells transfected with pre-miR-101. B. RLIP76 attenuates the suppressing effect of pre-miR-101 on cell growth. C. RLIP76 reverses the anti-proliferative effect of pre-miR-101 in RCC4 and 786-O cells. D. RLIP76 significantly abrogates pre-miR-101-induced apoptosis in ccRCC cells. E. RLIP76 significantly abolishes the inhibitory effect on cell migration of pre-miR-101 in RCC4 and 786-O cells. F. RLIP76 significantly attenuated the suppression of pre-miR-101 on cell invasion. **P<0.01.

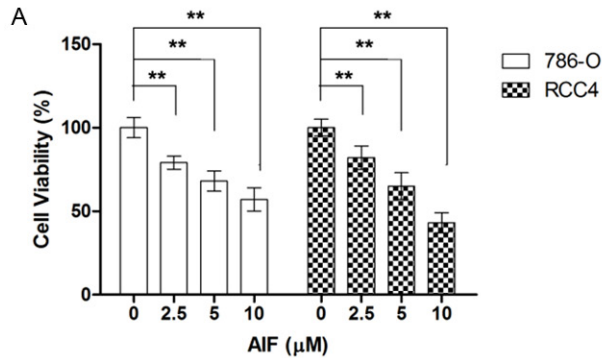
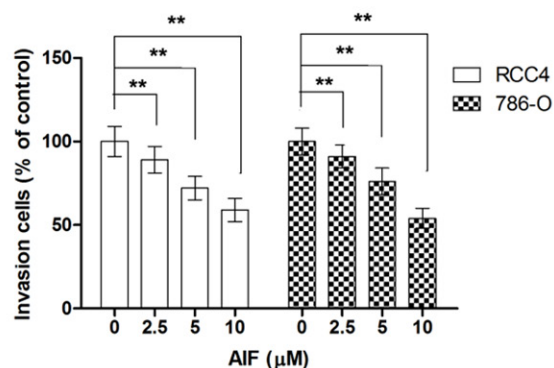
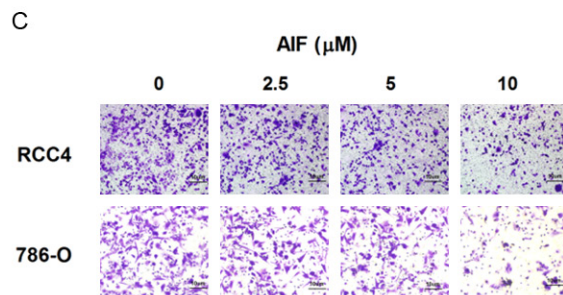
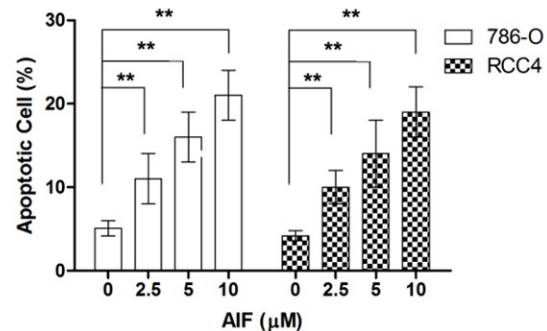
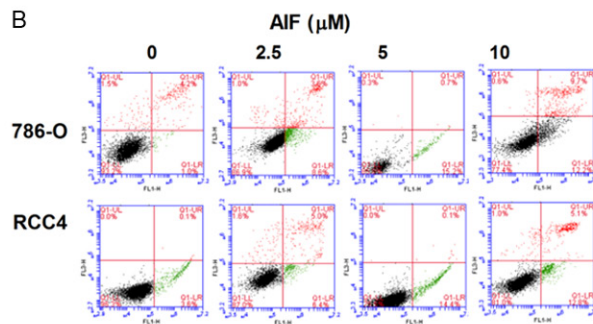


Figure 6. AIF suppresses cell growth, induces apoptosis and inhibits cell invasion in ccRCC. A. AIF suppresses cell growth in concentration-dependent manner. B. AIF increases the cell apoptosis in concentration-dependent manner. C. AIF inhibits cell invasion in concentration-dependent manner. **P<0.01.



apoptosis in both RCC4 and 786-O cells (Figure 6B). Besides suppressing cell growth and inducing apoptosis, AIF was also able to interfere with the invasion of ccRCC cells (Figure 6C).

AIF exerts anti-tumour effect through modulating miR-101/RLIP76 signalling by inhibiting Akt

Then, the mechanism by which AIF exerted its anti-tumor effect on ccRCC was investigated.

Given the facts that a number of flavonoids compounds exert anti-tumor effect by modulating miRNA expression, a miRNA array analysis was conducted to identify the potential miRNA target for AIF, which showed that miR-101 level was increased most by AIF treatment. To validate the results from miRNA array analysis, miR-101 level was examined in cells treated with different dosage of AIF. As shown in Figure 7, miR-101 level was increased by AIF treatment in a dose-dependent manner. As RLIP76 was a direct target of miR-101, the

Alpinumisoflavone suppress renal cell carcinoma

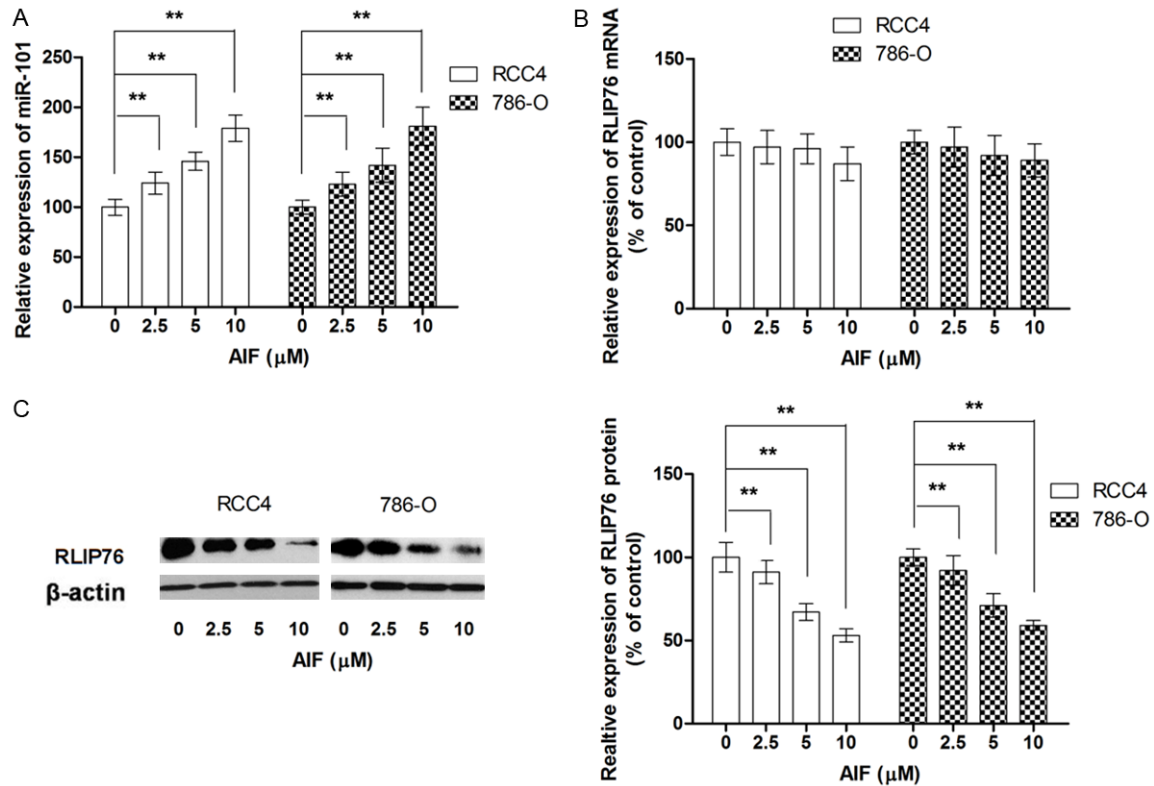


Figure 7. AIF regulates the expression of miR-101 and RLIP76. A. AIF increases the expression of miR-101 in concentration-dependent manner. B. AIF does not affect the expression of RLIP76 mRNA. C. AIF represses the protein expression of RLIP76 in concentration-dependent manner. ** $P < 0.01$.

effect of AIF on RLIP76 expression was also assessed. Although AIF was not able to cause marked change in mRNA level of RLIP76, AIF treatment resulted in a dose-dependent decrease in RLIP76 protein level. Moreover, our results showed that anti-miR-101 inhibitor or RLIP76 vector markedly reversed the loss of cell viability and apoptosis caused by AIF (Figure 8A and 8B). Correspondingly, anti-miR-101 or RLIP76 vector significantly rescued AIF-induced suppression on cell migration and invasion (Figure 8C and 8D). Collectively, our findings suggested that AIF exerted anti-tumor effect by modulating miR-101/RLIP76 signalling. Next, we conducted experiments to determine the upstream signalling responsible for the modulator effect of AIF on miR-101. Previous studies have showed that inhibition of Akt signalling in cancer cells resulted in up-regulation of miR-101 [26]. Hence, we postulated whether AIF increased miR-101 level in ccRCC cells by inhibiting Akt. As shown in Figure 8E, the ratio of phosphorylated Akt to total Akt was significantly decreased by AIF. In addition, we

also found the modulating effect of AIF on miR-101/RLIP76 was reversed by Akt activation IGF-1, suggesting that AIF modulates the expression of miR-101/RLIP76 through inhibiting Akt (Figure 8F).

AIF suppresses tumour growth and metastasis in vivo

To fully evaluate the anti-tumor effect of AIF, xenograft mice model was utilized. As shown in Figure 9A, AIF at both 40 and 80 mg/kg/day significantly delayed the growth of tumor. Immunohistochemistry analysis also showed that AIF treatment correlated with increased percentage of apoptotic tumor cells (Figure 9B). In consistent with in vitro results, RT-PCR and Simple Western analysis showed that AIF treatment in vivo led to increase in miR-101 expression while decrease in RLIP76 expression and p-Akt/t-Akt ratio (Figure 9C and 9D). Moreover, our results also confirmed that AIF was also able to suppressed pulmonary metastasis (Figure 9E).

Alpinumisoflavone suppress renal cell carcinoma

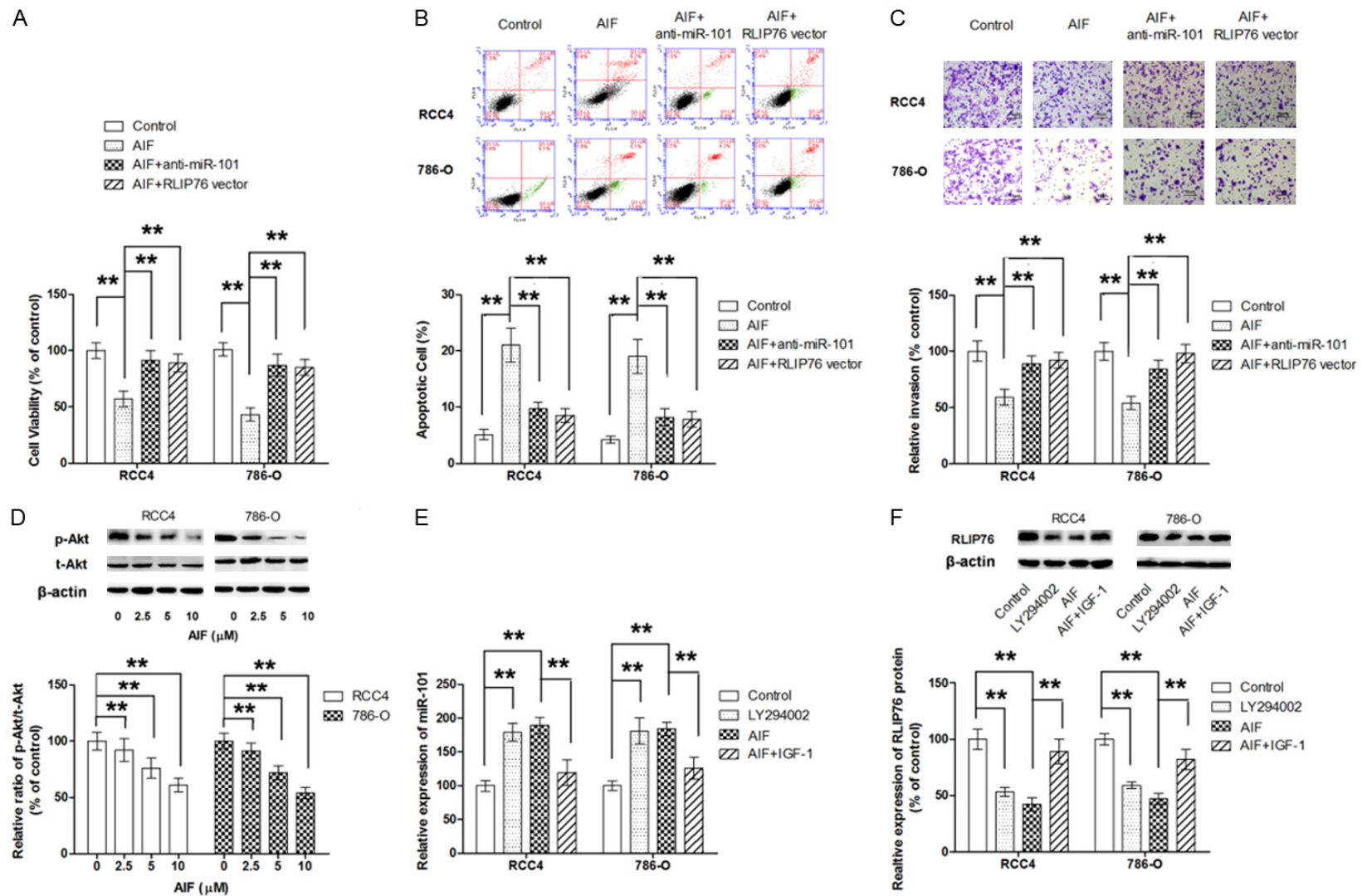


Figure 8. AIF exerts anti-tumor effect by modulating miR-101/RLIP76 through inhibiting Akt signaling. A. Anti-miR-101 and RLIP76 overexpression attenuates the suppressing effect of AIF on cell growth. B. Anti-miR-101 and RLIP76 overexpression attenuates the apoptosis-inducing effect of AIF in ccRCC cells. C. Anti-miR-101 and RLIP76 overexpression attenuates the inhibitory effect of AIF on cell invasion in ccRCC cells. D. AIF inhibits Akt signaling in concentration-dependent manner. E. Akt activator (IGF-1) significantly attenuated the modulating effect of AIF on miR-101 expression. F. Akt activator (IGF-1) significantly reverses the repressing effect of AIF on RLIP76 protein. **P<0.01.

Alpinumisoflavone suppress renal cell carcinoma

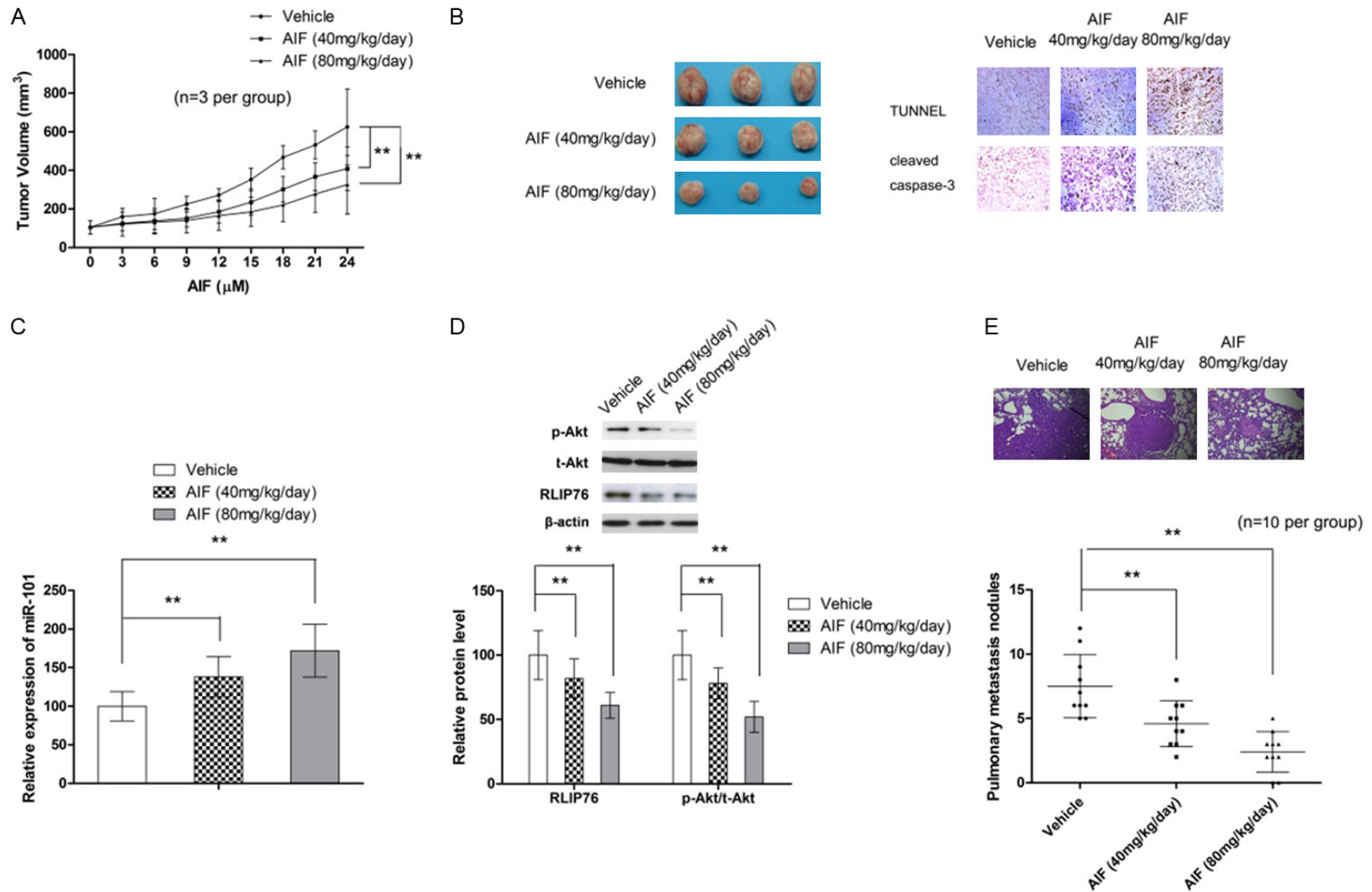


Figure 9. AIF suppresses tumor growth and metastasis in vivo. A. AIF suppresses tumor growth in vivo. B. AIF induces apoptosis in vivo. C. AIF increases the expression of miR-101 in xenograft tumor. D. AIF inhibits Akt signaling and represses RLIP76 expression in xenograft tumor. E. AIF suppresses pulmonary metastasis. ** $P < 0.01$.

Discussion

Lately, the use of natural products in cancer prevention and control has attracted a renewed interest. Epidemiological studies have also shown that high consumption of foods containing flavonoid compounds is associated with decreased risk of several types of human malignancies, implying the promising effect of these compound in cancer control [27]. In addition to the atheroprotective [17], estrogenic [18], anti-bacterial [19] activities, AIF, one of the flavonoid compound, has been found to have anti-cancer activities. In Lung cancer cells, AIF could induce cell death by repressing both the ERK/MAPK and NF- κ B pathways [21]. In this study, our results showed that AIF significant suppressed the tumor growth and metastasis of ccRCC both in vitro and in vivo. Moreover, our findings showed that the modulating effect of AIF on miR-101 mainly contributed to its anti-tumor effect in ccRCC.

As a family of endogenous, conserved, small non-coding RNA molecules with a length of 19-25 bp, MicroRNAs (miRNAs) regulate gene expression at the post-transcriptional level by binding to the partial sequence homology of the 3'-untranslated region of target messenger (m)RNA, resulting in translation inhibition or mRNA degradation. The role of miRNAs in human malignancies including ccRCC has been evaluated in a number of studies [28]. Studies by Yamasaki *et al* showed that both miR-138 and miR-218 suppressed cell migration and invasion in ccRCC cells in vitro [29, 30]. Let-7d has also been found to suppress RCC growth, metastasis and tumor macrophage infiltration by targeting COL3A1 and chemokine ligand-7 [31]. Other miRNAs such as miR-129-3p and miR-133b have also been identified as tumor suppressor and attenuate cell migration and invasion of RCC by downregulating multiple metastasis-associated genes [32, 33]. Collectively, these findings highlight the role of miRNAs in ccRCC oncogenesis and metastasis. As regards to miR-101, accumulating evidences showed that miR-101 plays an important functional role in numerous pathological progresses and may be used as a highly promising diagnostic and/or prognostic marker of human malignancies [34]. An early study by Sakurai *et al* also pointed out that miR-101 was significantly lower expressed in ccRCC cells and

ccRCC tissues compared with normal cells and non-timorous tissues, respectively [35], which suggested the role of miR-101 as tumor suppressor. This findings was backed up by a recent study, which also showed that miR-101 restoration in ccRCC cells could significantly suppressed cell proliferation and invasion [36]. In consistent with these previous studies, our results also showed that miR-101 was aberrantly downregulated in ccRCC tissues and the level of miR-101 inversely correlated with disease progression, further supporting the anti-tumor effect of miR-101 in ccRCC.

RLIP76 (DNP-SG ATPase) is a multi-functional protein involved in the ATP-dependent transport of glutathione conjugates and chemotherapy drugs [37-39]. Although the majority of early studies focused on the transporter activity of RLIP76, later evidence suggests that RLIP76 is involved in cell proliferation, metastasis and ligand-dependent receptor endocytosis [40-42]. Aberrant upregulation of RLIP76 has been detected in both cancer tissues and malignant cancer cells, which suggests the role of RLIP76 as oncogene [43-46]. In the context of ccRCC, RLIP76 functioned as an anti-apoptosis factor and mediated the drug-resistance to Sunitinib and Sorafenib [38]. However, the regulatory mechanism of RLIP76 in ccRCC cells remains unknown. In breast cancer cell, the promoter activity and expression of RLIP76 was regulated by p300, suggesting a transcriptional regulatory mechanism of RLIP76 [47]. A very recent study by Zhang *et* reported that RLIP76 is regulated by miR-124 at post-transcriptional level in melanoma cells [22]. In this study, our results showed that miR-101 exerted its anti-tumor by directly targeting RLIP76, highlighting the important role of post-transcriptional regulation in RLIP76 expression in cancer cells.

In conclusion, this present study showed that AIF suppressed tumor growth and metastasis by modulating miR-101/RLIP76 signaling.

Disclosure of conflict of interest

None.

Address correspondence to: Jie You, Shanghai Ninth People's Hospital, Shanghai JiaoTong University School of Medicine, Shanghai 200011, China. E-mail: youjieyj@163.com

References

- [1] Jemal A, Bray F, Center MM, Ferlay J, Ward E and Forman D. Global cancer statistics. *CA Cancer J Clin* 2011; 61: 69-90.
- [2] Gao H, Jiang Q, Han Y, Peng J and Wang C. Hispidulin potentiates the antitumor effect of sunitinib against human renal cell carcinoma in laboratory models. *Cell Biochem Biophys* 2015; 71: 757-764.
- [3] Rini BI, Campbell SC and Escudier B. Renal cell carcinoma. *Lancet* 2009; 373: 1119-1132.
- [4] Antonelli A, Cozzoli A, Zani D, Zanotelli T, Nicolai M, Cunico SC and Simeone C. The follow-up management of non-metastatic renal cell carcinoma: definition of a surveillance protocol. *BJU Int* 2007; 99: 296-300.
- [5] Escudier B, Eisen T, Stadler WM, Szczylik C, Oudard S, Siebels M, Negrier S, Chevreau C, Solska E, Desai AA, Rolland F, Demkow T, Hutson TE, Gore M, Freeman S, Schwartz B, Shan M, Simantov R, Bukowski RM; TARGET Study Group. Sorafenib in advanced clear-cell renal-cell carcinoma. *N Engl J Med* 2007; 356: 125-134.
- [6] Hudes G, Carducci M, Tomczak P, Dutcher J, Figlin R, Kapoor A, Staroslawska E, Sosman J, McDermott D, Bodrogi I, Kovacevic Z, Lesovoy V, Schmidt-Wolf IG, Barbarash O, Gokmen E, O'Toole T, Lustgarten S, Moore L, Motzer RJ and Global AT. Temsirolimus, interferon alfa, or both for advanced renal-cell carcinoma. *N Engl J Med* 2007; 356: 2271-2281.
- [7] Motzer RJ, Hutson TE, Tomczak P, Michaelson MD, Bukowski RM, Rixe O, Oudard S, Negrier S, Szczylik C, Kim ST, Chen I, Bycott PW, Baum CM and Figlin RA. Sunitinib versus interferon alfa in metastatic renal-cell carcinoma. *N Engl J Med* 2007; 356: 115-124.
- [8] Motzer RJ, Escudier B, Oudard S, Hutson TE, Porta C, Bracarda S, Grunwald V, Thompson JA, Figlin RA, Hollaender N, Urbanowitz G, Berg WJ, Kay A, Lebwohl D, Ravaud A; RECORD-1 Study Group. Efficacy of everolimus in advanced renal cell carcinoma: a double-blind, randomised, placebo-controlled phase III trial. *Lancet* 2008; 372: 449-456.
- [9] Ventura A and Jacks T. MicroRNAs and cancer: short RNAs go a long way. *Cell* 2009; 136: 586-591.
- [10] Wu GQ, Chai KQ, Zhu XM, Jiang H, Wang X, Xue Q, Zheng AH, Zhou HY, Chen Y, Chen XC, Xiao JY, Ying XH, Wang FW, Rui T, Liao YJ, Xie D, Lu LQ and Huang DS. Anti-cancer effects of curcumin on lung cancer through the inhibition of EZH2 and NOTCH1. *Oncotarget* 2016; 7: 26535-26550.
- [11] Liu J, Pang Y, Wang H, Li Y, Sun X, Xu F, Ren H and Liu D. [miR-101 inhibits the proliferation and migration of breast cancer cells via down-regulating the expression of DNA methyltransferase 3a]. *Xi Bao Yu Fen Zi Mian Yi Xue Za Zhi* 2016; 32: 299-303.
- [12] Slattery ML, Herrick JS, Pellatt DF, Mullany LE, Stevens JR, Wolff E, Hoffman MD, Wolff RK and Samowitz W. Site-specific associations between miRNA expression and survival in colorectal cancer cases. *Oncotarget* 2016; 7: 60193-60205.
- [13] Long Y, Wu Z, Yang X, Chen L, Han Z, Zhang Y, Liu J, Liu W and Liu X. MicroRNA-101 inhibits the proliferation and invasion of bladder cancer cells via targeting c-FOS. *Mol Med Rep* 2016; 14: 2651-2656.
- [14] Chakravarthi BV, Goswami MT, Pathi SS, Robinson AD, Cieslik M, Chandrashekar DS, Agarwal S, Siddiqui J, Daignault S, Carskadon SL, Jing X, Chinnaiyan AM, Kunju LP, Palanisamy N and Varambally S. MicroRNA-101 regulated transcriptional modulator SUB1 plays a role in prostate cancer. *Oncogene* 2016; 35: 6330-6340.
- [15] Yang J, Lu Y, Lin YY, Zheng ZY, Fang JH, He S and Zhuang SM. Vascular mimicry formation is promoted by paracrine TGF-beta and SDF1 of cancer-associated fibroblasts and inhibited by miR-101 in hepatocellular carcinoma. *Cancer Lett* 2016; 383: 18-27.
- [16] Chen DL, Ju HQ, Lu YX, Chen LZ, Zeng ZL, Zhang DS, Luo HY, Wang F, Qiu MZ, Wang DS, Xu DZ, Zhou ZW, Pelicano H, Huang P, Xie D, Wang FH, Li YH and Xu RH. Long non-coding RNA XIST regulates gastric cancer progression by acting as a molecular sponge of miR-101 to modulate EZH2 expression. *J Exp Clin Cancer Res* 2016; 35: 142.
- [17] Mvondo MA, Njamen D, Kretschmar G, Imma Bader M, Tanee Fomum S, Wandji J and Vollmer G. Alpinumisoflavone and abyssinone V 4'-methylether derived from *Erythrina lysistemon* (Fabaceae) promote HDL-cholesterol synthesis and prevent cholesterol gallstone formation in ovariectomized rats. *J Pharm Pharmacol* 2015; 67: 990-996.
- [18] Mvondo MA, Njamen D, Tanee Fomum S and Wandji J. Effects of alpinumisoflavone and abyssinone V-4'-methyl ether derived from *Erythrina lysistemon* (Fabaceae) on the genital tract of ovariectomized female Wistar rat. *Phytother Res* 2012; 26: 1029-1036.
- [19] Chukwujekwu JC, Van Heerden FR and Van Staden J. Antibacterial activity of flavonoids from the stem bark of *Erythrina caffra* thunb. *Phytother Res* 2011; 25: 46-48.
- [20] Kuete V, Mbaveng AT, Nono EC, Simo CC, Zeino M, Nkengfack AE and Efferth T. Cytotoxicity of seven naturally occurring phenolic compounds towards multi-factorial drug-resistant cancer cells. *Phytomedicine* 2016; 23: 856-863.

Alpinumisoflavone suppress renal cell carcinoma

- [21] Namkoong S, Kim TJ, Jang IS, Kang KW, Oh WK and Park J. Alpinumisoflavone induces apoptosis and suppresses extracellular signal-regulated kinases/mitogen activated protein kinase and nuclear factor-kappaB pathways in lung tumor cells. *Biol Pharm Bull* 2011; 34: 203-208.
- [22] Zhang D, Han Y and Xu L. Upregulation of miR-124 by physcion 8-O-beta-glucopyranoside inhibits proliferation and invasion of malignant melanoma cells via repressing RLIP76. *Biomed Pharmacother* 2016; 84: 166-176.
- [23] Lewis BP, Shih IH, Jones-Rhoades MW, Bartel DP and Burge CB. Prediction of mammalian microRNA targets. *Cell* 2003; 115: 787-798.
- [24] John B, Enright AJ, Aravin A, Tuschl T, Sander C and Marks DS. Human MicroRNA targets. *PLoS Biol* 2004; 2: e363.
- [25] Liao W, Liu W, Yuan Q, Liu X, Ou Y, He S, Yuan S, Qin L, Chen Q, Nong K, Mei M and Huang J. Silencing of DLGAP5 by siRNA significantly inhibits the proliferation and invasion of hepatocellular carcinoma cells. *PLoS One* 2013; 8: e80789.
- [26] Ferreira AC, Robaina MC, Rezende LM, Severino P and Klumb CE. Histone deacetylase inhibitor prevents cell growth in Burkitt's lymphoma by regulating PI3K/Akt pathways and leads to upregulation of miR-143, miR-145, and miR-101. *Ann Hematol* 2014; 93: 983-993.
- [27] Xie J, Gao H, Peng J, Han Y, Chen X, Jiang Q and Wang C. Hispidulin prevents hypoxia-induced epithelial-mesenchymal transition in human colon carcinoma cells. *Am J Cancer Res* 2015; 5: 1047-1061.
- [28] Filipowicz W, Bhattacharyya SN and Sonenberg N. Mechanisms of post-transcriptional regulation by microRNAs: are the answers in sight? *Nat Rev Genet* 2008; 9: 102-114.
- [29] Yamasaki T, Seki N, Yamada Y, Yoshino H, Hidaka H, Chiyomaru T, Nohata N, Kinoshita T, Nakagawa M and Enokida H. Tumor suppressive microRNA138 contributes to cell migration and invasion through its targeting of vimentin in renal cell carcinoma. *Int J Oncol* 2012; 41: 805-817.
- [30] Yamasaki T, Seki N, Yoshino H, Itesako T, Hidaka H, Yamada Y, Tatarano S, Yonezawa T, Kinoshita T, Nakagawa M and Enokida H. MicroRNA-218 inhibits cell migration and invasion in renal cell carcinoma through targeting caveolin-2 involved in focal adhesion pathway. *J Urol* 2013; 190: 1059-1068.
- [31] Su B, Zhao W, Shi B, Zhang Z, Yu X, Xie F, Guo Z, Zhang X, Liu J, Shen Q, Wang J, Li X, Zhang Z and Zhou L. Let-7d suppresses growth, metastasis, and tumor macrophage infiltration in renal cell carcinoma by targeting COL3A1 and CCL7. *Mol Cancer* 2014; 13: 206.
- [32] Chen X, Ruan A, Wang X, Han W, Wang R, Lou N, Ruan H, Qiu B, Yang H and Zhang X. miR-129-3p, as a diagnostic and prognostic biomarker for renal cell carcinoma, attenuates cell migration and invasion via downregulating multiple metastasis-related genes. *J Cancer Res Clin Oncol* 2014; 140: 1295-1304.
- [33] Wu D, Pan H, Zhou Y, Zhou J, Fan Y and Qu P. microRNA-133b downregulation and inhibition of cell proliferation, migration and invasion by targeting matrix metalloproteinase-9 in renal cell carcinoma. *Mol Med Rep* 2014; 9: 2491-2498.
- [34] Zhao H, Tang H, Huang Q, Qiu B, Liu X, Fan D, Gong L, Guo H, Chen C, Lei S, Yang L, Lu J and Bao G. MiR-101 targets USP22 to inhibit the tumorigenesis of papillary thyroid carcinoma. *Am J Cancer Res* 2016; 6: 2575-2586.
- [35] Sakurai T, Bilim VN, Ugolkov AV, Yuuki K, Tsukigi M, Motoyama T and Tomita Y. The enhancer of zeste homolog 2 (EZH2), a potential therapeutic target, is regulated by miR-101 in renal cancer cells. *Biochem Biophys Res Commun* 2012; 422: 607-614.
- [36] Goto Y, Kurozumi A, Nohata N, Kojima S, Matsushita R, Yoshino H, Yamazaki K, Ishida Y, Ichikawa T, Naya Y and Seki N. The microRNA signature of patients with sunitinib failure: regulation of UHRF1 pathways by microRNA-101 in renal cell carcinoma. *Oncotarget* 2016; 7: 59070-59086.
- [37] Singhal SS, Singhal J, Nair MP, Lacko AG, Awasthi YC and Awasthi S. Doxorubicin transport by RALBP1 and ABCG2 in lung and breast cancer. *Int J Oncol* 2007; 30: 717-725.
- [38] Singhal SS, Sehrawat A, Sahu M, Singhal P, Vatsyayan R, Rao Lelsani PC, Yadav S and Awasthi S. Rlip76 transports sunitinib and sorafenib and mediates drug resistance in kidney cancer. *Int J Cancer* 2010; 126: 1327-1338.
- [39] Singhal SS, Sehrawat A, Mehta A, Sahu M and Awasthi S. Functional reconstitution of RLIP76 catalyzing ATP-dependent transport of glutathione-conjugates. *Int J Oncol* 2009; 34: 191-199.
- [40] Yadav S, Zajac E, Singhal SS, Singhal J, Drake K, Awasthi YC and Awasthi S. POB1 over-expression inhibits RLIP76-mediated transport of glutathione-conjugates, drugs and promotes apoptosis. *Biochem Biophys Res Commun* 2005; 328: 1003-1009.
- [41] Singhal SS, Yadav S, Vatsyayan R, Chaudhary P, Borvak J, Singhal J and Awasthi S. Increased expression of cdc2 inhibits transport function of RLIP76 and promotes apoptosis. *Cancer Lett* 2009; 283: 152-158.
- [42] Hu Y and Mivechi NF. HSF-1 interacts with Ral-binding protein 1 in a stress-responsive, multi-

Alpinumisoflavone suppress renal cell carcinoma

- protein complex with HSP90 in vivo. *J Biol Chem* 2003; 278: 17299-17306.
- [43] Singhal SS, Singhal J, Yadav S, Sahu M, Awasthi YC and Awasthi S. RLIP76: a target for kidney cancer therapy. *Cancer Res* 2009; 69: 4244-4251.
- [44] Singhal SS, Singhal J, Yadav S, Dwivedi S, Boor PJ, Awasthi YC and Awasthi S. Regression of lung and colon cancer xenografts by depleting or inhibiting RLIP76 (Ral-binding protein 1). *Cancer Res* 2007; 67: 4382-4389.
- [45] Singhal SS, Roth C, Leake K, Singhal J, Yadav S and Awasthi S. Regression of prostate cancer xenografts by RLIP76 depletion. *Biochem Pharmacol* 2009; 77: 1074-1083.
- [46] Wang Q, Wang JY, Zhang XP, Lv ZW, Fu D, Lu YC, Hu GH, Luo C and Chen JX. RLIP76 is overexpressed in human glioblastomas and is required for proliferation, tumorigenesis and suppression of apoptosis. *Carcinogenesis* 2013; 34: 916-926.
- [47] Sehrawat A, Yadav S, Awasthi YC, Basu A, Warden C and Awasthi S. P300 regulates the human RLIP76 promoter activity and gene expression. *Biochem Pharmacol* 2013; 85: 1203-1211.